

# Comparative analysis of diagnostic platforms for measurement of differentially methylated insulin DNA

Ryan J. Farr<sup>1†</sup>, Wilson K. M. Wong<sup>1</sup>, Cody-lee Maynard<sup>1</sup>, Sarah A. Tersey<sup>2</sup>, Raghavendra G. Mirmira<sup>2</sup>, Anandwardhan A. Hardikar<sup>1\*</sup>, Mugdha V. Joglekar<sup>1\*</sup>

<sup>1</sup>Diabetes and Islet Biology Group, NHMRC Clinical Trials Centre, Faculty of Medicine, The University of Sydney, Level 6, Medical Foundation Building, 92-94 Parramatta Road, Camperdown, NSW 2050, Australia

<sup>2</sup>Herman B Wells Center for Pediatric Research, Center for Diabetes and Metabolic Diseases, and Department of Pediatrics, Indiana University School of Medicine, Indianapolis, IN 46202, USA

<sup>†</sup>Current address: Pathology and Pathogenesis Group, Diagnostics, Surveillance and Response, Australian Animal Health Laboratory, Commonwealth Scientific and Industrial Research Organization (CSIRO), 5 Portarlington Road, Geelong 3220, Australia

\*Correspondence author: Anandwardhan A. Hardikar, Email: anand.hardikar@ctc.usyd.edu.au; or Mugdha V. Joglekar, Email: mugdha.joglekar@ctc.usyd.edu.au

Competing interests: The authors have declared that no competing interests exist.

Abbreviations used: cfDNA, cell-free DNA; CVs, coefficients of variation; QS3D, QuantStudio 3D; T1D, type 1 diabetes

Received November 20, 2018; Revision received January 16, 2019; Accepted February 8, 2019; Published June 3, 2019

## ABSTRACT

Circulating cell-free DNA (cfDNA) has been intensively investigated as a diagnostic and prognostic marker for various cancers. In recent years, presence of unmethylated insulin cfDNA in the circulation has been correlated with pancreatic  $\beta$ -cell death and risk of developing type 1 diabetes. Digital (d)PCR is an increasingly popular method of quantifying insulin cfDNA due to its ability to determine absolute copy numbers, and its increased sensitivity when compared to the more routinely used quantitative PCR. Multiple platforms have been developed to carry out dPCR. However, not all technologies perform comparably, thereby necessitating evaluation of each platform. Here, we compare two dPCR platforms: the QuantStudio 3D (QS3D, Applied Biosystems) and the QX200 (Bio-Rad), to measure copies of unmethylated/methylated insulin plasmids. The QS3D detected greater copy numbers of the plasmids than the QX200 (manual mode), whereas QX200 demonstrated minimal replicate variability, increased throughput, ease of use and the potential for automation. Overall, the performance of QX200, in our hands, was better suited to measure differentially methylated insulin cfDNA.

**Keywords:** digital PCR; unmethylated insulin; cell free DNA; type 1 diabetes; diagnostic biomarker

## INTRODUCTION

The concept of circulating cell-free DNA (cfDNA) as a biomarker is well established in the area of cancer biology [1-3]. It utilizes a less invasive method of assessing an individual's health status using liquid biopsy (*e.g.*, blood, plasma, urine) samples. In the progression to type 1 diabetes (T1D), immune-mediated loss of insulin-producing  $\beta$ -cells starts much earlier than the clinical diagnosis of the disease [4]. This trend of gradual  $\beta$ -cell death suggests that detection of  $\beta$ -cell-specific cfDNA has great potential as a biomarker of T1D progression.

Despite having an identical genome, each cell type within the body contains DNA with a unique methylation pattern that reflects upon their specific gene expression profile. The insulin gene, including the promoter region, is typically unmethylated within the pancreatic  $\beta$ -cells, but methylated in almost all other cell types, thereby providing a strong rationale to develop assays to quantify methylated and unmethylated

insulin DNA as a measure of islet  $\beta$ -cell death [5-10]. These studies have used different methods including nested PCR, TaqMan multiplex PCR, digital PCR (dPCR) and sequencing to measure circulating unmethylated insulin cfDNA.

dPCR is becoming an increasingly popular method of quantifying nucleic acids as it is able to provide absolute quantitation of target gene/transcript copies, thereby offering a more sensitive and absolutely quantifiable technology than conventional real-time qPCR and other existing technologies [11-14]. cfDNA is often present in low levels within circulation, making it difficult to detect *via* other molecular methods thus favoring dPCR due to its robust and sensitive nature. It is a technological refinement of qPCR that is achieved by splitting the clonal amplification into thousands of distinct reactions. By reading the fluorescence of each of these reactions as positive (the sequence of interest is present) or negative (no sequence of interest), digital PCR can apply the Poisson distribution to calculate the absolute copy num-

**How to cite this article:** Farr RJ, Wong WKM, Maynard C, Tersey SA, Mirmira RG, Hardikar AA, Joglekar MV. Comparative analysis of diagnostic platforms for measurement of differentially methylated insulin DNA. *J Biol Methods* 2019;6(2):e113. DOI: 10.14440/jbm.2019.280

ber of the sequence of interest. Various studies have used dPCR as a quantitative tool for gene detection in different diseases such as diabetes [7], cancer [15], and infectious diseases [16]. Like any other technique, multiple platforms including the Droplet Digital™ PCR system (Bio-Rad), the RainDrop® Digital PCR system (RainDance Technologies) and QuantStudio® 3D Digital PCR system (Life Technologies) have been developed to utilize it and these must be compared to ensure robust reproducibility and ease of use.

Present study evaluates two digital PCR platforms: the QuantStudio® 3D (QS3D, Applied Biosystems) and the QX200 Droplet Digital™ (QX200, Bio-Rad) to measure unmethylated and methylated insulin cfDNA. The QS3D uses a finely-crafted chip with 20000, equally sized, nanoscale reaction wells to partition the amplification reaction. The QX200 system relies on a droplet generator that splits the PCR reaction in up to 20000 aqueous droplets within the emulsion oil. The reproducibility of each platform was assessed using mixtures of methylated and unmethylated insulin DNA plasmids. This step was essential before analyzing the actual samples from individuals with and without T1D.

## MATERIALS AND METHODS

### Plasmids

Unmethylated (UM) and methylated (M) Ins plasmids [7] were amplified by transfecting into MAX Efficiency® DH5α™ Competent Cells (Thermo Fisher), and selected by using 50 µg/ml ampicillin. Plasmids were purified using the ZymoPURE Plasmid Midi Prep DNA Isolation Kit (Zymo Research). Purified plasmids (3.9 kB) were combined to create solutions with varying percentages of each unmethylated (UM) and methylated (M) plasmids. The percentages used were 100%, 99.9%, 99%, 90%, 75%, 50%, 25%, 10% and 0%. Each mixture had the remaining volumes made up with the percentage of other plasmid (*i.e.*, the 90% UM plasmid solution had 10% M plasmid). Each solution had a total final concentration of 0.5 pg/µl. In order to better visualize these results, data for four dilutions (99.9:0.1 and 99.0:1.0 for both methylated and unmethylated plasmids) were not included in figures.

### Digital PCR

Digital PCR was performed as per the method described in the article by Fisher *et al.* [7]. Each plasmid mixture (as described above) and a no template control (NTC) were run in triplicate. The digital PCR reactions were as follows: 1× QuantStudio 3D Digital PCR Mastermix v2 (Applied Biosystems) or 1× ddPCR Supermix for Probes (No dUTP) (Bio-Rad), 1× Custom TaqMan SNP assay AH21BH1, 10U EcoR1, nuclease-free water and 0.5 pg (1 µl) of the plasmid mix. Total reaction volume for the QS3D was 14.5 µl, while total reaction volume for the QX200 was 20 µl as per the manufacturer's recommendations. Detailed compositions are presented in **Table 1**. Partitioning of PCR reaction was achieved using manual droplet generation (Bio-Rad) or nanofluidic chip loading (Applied Biosystems) as per the respective manufacturer's protocol. Once the reactions were partitioned, they were amplified using the following cycling conditions: 95°C for 10 min, 40 cycles (94°C for 30 s, 57.5°C for 1 min), 98°C for 10 min, 12°C hold. The ramp rate for thermocycling condition was set to 2°C/s for all steps. After PCR, each nanofluidic chip was placed face-up and read separately (one at a time) in the QS3D. Each chip analysis took < 30 s. The QS3D captured the ROX, FAM, and VIC fluorescence of each well on the chip, with ROX

used as a passive dye to ensure sample loading. On the other hand, the PCR amplified droplets from QX200 generator were read from one well at a time by streamlining them into a single file that passes through a two-color optical detection system on the QX200 Droplet Reader.

### Statistics

Plasmid dilutions were assayed in triplicate for each of the dPCR experiments performed on the QS3D and QX200 platforms. Pearson correlation coefficients and two-tailed *P* values were calculated using GraphPad Prism 7 software. *P* value of < 0.05 was considered significant in the group-wise comparisons.

**Table 1. Composition of mastermix for digital PCR reactions.**

	QS3D (µl/reaction)	QX200 (µl/reaction)
QuantStudio 3D digital PCR Mastermix v2 (2 ×)	7.25	-
ddPCR Supermix for Probes (No dUTP) (2 ×)	-	10
Custom TaqMan SNP assay AH21BH1 (20 ×)	0.725	1
20 U/µl EcoR1	0.5	0.5
Nuclease free water	5.025	7.5
0.5 pg of the plasmid mix	1	1
Total	14.5	20

Table 1 presents volumes of each component to be added in the mastermix for digital PCR reaction on each platform. Final volumes are calculated based on the number of reactions to be run and always calculating for 5% extra reactions to account for pipetting errors.

## RESULTS

### Overview of digital PCR platforms

**Figure S1** presents an overview of the two dPCR technologies (QS3D and QX200) that are compared here.

QS3D system uses a chip that has 20000 wells etched on a silicon substrate with each well of a maximum width of 60 µm (S1A), while the QX200 generates up to the same number of droplets by mixing the PCR reaction in oil (S1B) either manually or using an automated droplet generator. After partitioning the PCR mix, end-stage PCR is performed and then the PCR product is analyzed for presence of different fluorescent probes as described in the methods. Once the dPCR reactions have been completed, a threshold must be placed on both the FAM and VIC fluorescence to determine partitions that separate amplified products that are negative for both probes, positive for a single probe, or those that are positive for both probes. **Figure S1C** and **S1D** show representative plots of these thresholds on both platforms. The identification of these populations varies on the QS3D platform, resulting in an overlay with no discernible populations (**Fig. S1C**), which makes it difficult to set up the same threshold for multiple samples using the QS3D platform. On the other hand, the QX200 consistently separates droplets into four distinct populations (**Fig. S1D**).

### Accuracy of the data on both dPCR platforms

The plasmid mixtures were analyzed on both dPCR platforms, and their absolute copy numbers were determined (Fig. 1A and 1B).

None of the platforms were able to detect insulin cfDNA plasmids with 100% efficiency. The QS3D platform, however, demonstrated a 1.8-fold higher insulin cfDNA copy number (Fig. 1A) than that detected on the QX200 platform (Fig. 1B). The mixing ratios of the unmethylated and methylated insulin plasmids were correctly reflected on both

the platforms. We then plotted expected and observed percentages of mixtures for both the plasmids (Fig. 1C and 1D). Although data obtained from both platforms show a preferential expression of methylated insulin plasmid in all combinations and on both the platforms, both the unmethylated and methylated insulin plasmids demonstrated a very good correlation with Pearson  $r = 0.9958$  and  $P < 0.0001$  on QS3D and Pearson  $r = 0.9954$  and  $P < 0.0001$  on QX200 between expected and observed ratios for the two plasmids.

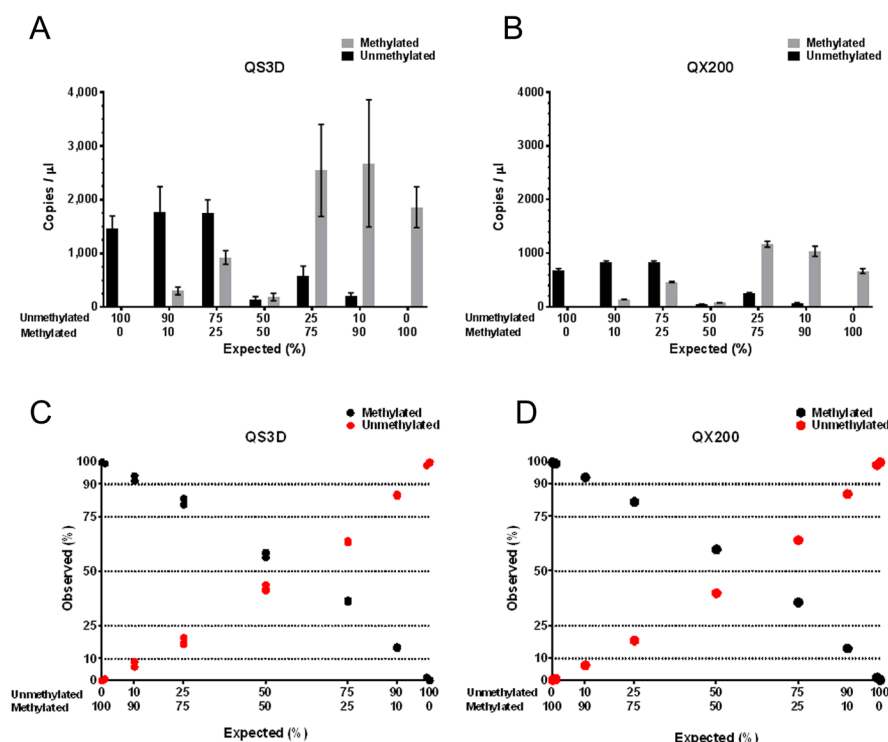


**Figure 1. Quantification of unmethylated and methylated insulin DNA.** Mixtures containing different proportions of unmethylated and methylated insulin plasmids (presented on X axis) were analyzed on the QS3D and QX200 dPCR platforms. Absolute copy numbers (copies/μl) generated from these different combinations on QS3D (A) and QX200 (B) platforms are presented as mean  $\pm$  SD. We then plotted expected versus observed percentages of unmethylated and methylated insulin plasmid mixtures on QS3D (C) and QX200 (D) platforms. Each plasmid mixture was run in triplicate. Dotted lines are expected percentages.

### Reproducibility of measurements on both the dPCR platforms

Both the platforms are designed to partition the PCR reaction into around 20000 individual reactions for PCR. During normal operation, however, neither of these platforms utilized the maximum 20000 partitions. Rather, the QS3D employed  $17300 \pm 624.3$  (mean  $\pm$  SD) wells and the QX200 generated  $16524 \pm 1863$  (mean  $\pm$  SD) usable droplets (Fig. 2A).

Whilst both platforms had enough partitions to estimate absolute copy numbers, the QS3D demonstrated more consistent partitioning. When the coefficients of variation (CVs) were determined for multiple measurements of both unmethylated and methylated insulin plasmids, we observed that QS3D demonstrated a higher level of variability for both the plasmids with significantly higher assay CVs than the QX200 platform (Fig. 2B). Finally, when NTCs were analyzed on the dPCR platforms, the QS3D detected DNA copies more frequently than the QX200 (Fig. 2C).

### DISCUSSION

Digital PCR offers a major advantage over other PCR technologies by enabling absolute quantitation of transcript copy numbers. Although a favored method of quantitating low levels of circulating cfDNA, the choice of technology can heavily influence the generation and reproducibility of such data [17]. We therefore directly compared two currently available dPCR platforms; the QS3D and the QX200.

We find that the absolute copy number values are always higher on the QS3D platform (Fig. 1A) as compared to QX200 (Fig. 1B). None of the platforms could detect the actual plasmid copy numbers. QS3D was seen to measure 1.8-fold more copies than the QX200 platform, although it also presented with 3- to 6-fold higher copy numbers in the NTC reactions (Fig. 2C). Our analysis identified QX200 dPCR system offering higher reproducibility (Fig. 2B).

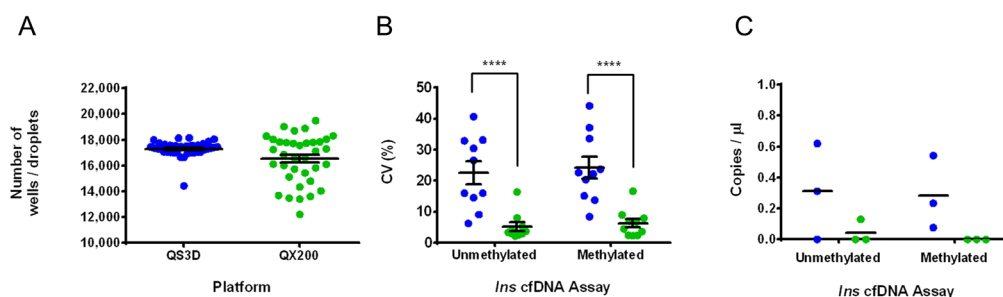


**Figure 2. Accuracy and reproducibility for manual processing workflows across the two platforms.** Number of partitions created on both platforms. Scatterplot showing the number of wells (QS3D, blue) or droplets (QX200, green) utilized for the calculation of absolute DNA copy numbers. Data were generated from  $N = 36$  per group and presented as mean  $\pm$  SEM (A). CVs were calculated for each dPCR platform and their distribution for unmethylated and methylated assays is shown (B). Data on QS3D (blue) and QX200 (green) platforms are compared as mean  $\pm$  SEM. NTC was run in triplicate on the QS3D (blue) and QX200 (green) platforms and absolute copies are presented in (C) with solid line at mean. \*\*\*\* $P < 0.0001$ .

**Table 2. Comparative analysis of two digital PCR platforms.**

	QS3D	QX200
Min. samples/run	1	8
Samples/8 h (average/max)	24/48	96/192
Detection range (copies/ $\mu$ l)	200–2000	0.25–5000
Supported dye(s)	FAM, VIC and ROX*	FAM, HEX (or VIC), EvaGreen (or SYBR green)
Time to load one sample (min)	5	1
Time to read one sample (min)	0.5	1.5–2
Ease of loading	++	+++
Ease of analysis	++	+++
Possibility of automation	No	Yes
Possibility of aerosolic cross-contamination	Low	High
Cost per sample	\$\$\$	\$\$

Table 2 presents a comparison between QS3D and QX200 platforms in regards to different parameters such as number of samples, loading time, ease of handling and ease of analysis. The number of “+” or “\$” signs indicate the process being easier (more +s) or more expensive (more \$s) than the other. \*Serve as a reference detection only.

Several other parameters were also compared between the two dPCR platforms (Table 2).

Theoretically one sample can be run at a time on QS3D. However, the included reagents necessitate multiples of four samples to be processed on the QS3D, so as to avoid reagent wastage and achieve cost efficiency. It may not be necessary to run positive/negative controls every time on QS3D, as each sample is loaded and analyzed separately; however, it is always better to include controls to ensure assay validity and appropriate separation of populations. QX200 needs at least eight samples per run and there should be a positive and negative control per run to determine the threshold. The loading of the QS3D chip takes longer time as compared to the QX200 platform; however, QS3D chip is read in 30 s, whereas the whole 96 well plate on a droplet reader is completed in just over two hours ( $> 1$  min per sample). QS3D being a closed system has minimal chances of aerosolic contamination, which is more likely on QX200 platform. The QX200 is a high throughput platform designed for parallel processing of up to 96 samples at a time, whilst the QS3D platform has been designed for low sample throughput

workflows. The throughput of QX200 platform can be further expanded utilizing an automated droplet generator, which not only improves droplet numbers but also the assay reproducibility. This is also one of the major reasons for QX200 as a preferred platform to undertake cfDNA quantitation, particularly in large clinical studies.

There have been previous studies where different platforms are compared for cfDNA quantification [18–21]. Four different digital PCR platforms (BioMark, QX100, QuantStudio 12k and RainDrop) were evaluated for accuracy and measurement uncertainty for known copies of a plasmid DNA [18]. It was reported that all the four platforms perform equally well in terms of reporting the plasmid concentration within the expected range. This report however does not have any evaluation of the QS3D platform. Later in another report, QS3D and QX100 were compared to observe that QX100 was better in terms of accuracy and efficiency with less measurement bias than QS3D [20]. Unlike this report, we find that the measurement bias between the expected values and observed values for unmethylated and methylated insulin plasmids was similar on both QX200 and QS3D platforms. There is one other



comparison evaluating only QS3D and QX200 for detecting donor cfDNA in acute kidney transplant recipients [21]. This study reported QX200 to be better in terms of accuracy and sensitivity for detecting donor cfDNA in urine samples of kidney transplant recipients.

Our analysis represents the only comparative study for insulin cfDNA measurement using dPCR platforms. This is an important area of research wherein the copy number of insulin cfDNA can be used to predict the progression to T1D, to assess treatment efficacies of drugs that are aimed to retard the death of insulin-producing cells and to estimate the success of islet transplant procedures by assessing the death of insulin-producing cells in T1D individuals transplanted with cadaveric donor islets. Since different dPCR systems can provide varying estimates, a direct comparison of the two systems becomes necessary. One of the limitations is that the current study did not involve comparison with other available systems offering absolute quantitation of gene transcripts/DNA. However, the QS3D and QX200 are two of the most popular systems available to the scientific community and our study presents the comparative analysis for researchers aiming to use digital PCR platforms for diabetes research. As discussed above, each of the two platforms have their own strengths and limitations, which we hope would be useful for individual researchers to select for their own study.

## Acknowledgments

The support provided to Farr RJ and Wong WKM through Australian Government's post-graduate and the University of Sydney post-graduate awards, Joglekar MV through the Australian Diabetes Society (ADS) Skip Martin fellowship and currently through the JDRF International post-doctoral fellowship, Maynard C through NHMRC clinical Trials Centre and to Hardikar AA through the ARC Future Fellowship and currently through the JDRF Australia Career Development Award as well as the visiting professorship through the Danish Diabetes Academy is highly acknowledged. Mirmira RG acknowledges funding from NIH grant R01 DK60581. The authors acknowledge the infrastructure support provided to Hardikar AA through the NHMRC Clinical Trials Center, JDRF Australia, The University of Sydney and the Rebecca Cooper Medical Research Foundation.

## Author contributions

Farr RJ performed experiments and analyzed the data. Joglekar MV analyzed data and wrote the first manuscript draft. Wong WKM and Maynard C assisted in experimentation. Tersey SA and Mirmira RG designed the plasmids and contributed to writing this draft. Hardikar AA and Joglekar MV designed and planned the study and wrote the final draft. All authors agreed on the final revised draft.

## References

1. Aarthi R, Mani S, Velusami S, Sundarsingh S, Rajkumar T (2015) Role of Circulating Cell-Free DNA in Cancers. *Mol Diagn Ther* 19: 339-350. doi: [10.1007/s40291-015-0167-y](https://doi.org/10.1007/s40291-015-0167-y). PMID: [26400814](https://pubmed.ncbi.nlm.nih.gov/26400814/)
2. Francis G, Stein S (2015) Circulating Cell-Free Tumour DNA in the Management of Cancer. *Int J Mol Sci* 16: 14122-14142. doi: [10.3390/ijms160614122](https://doi.org/10.3390/ijms160614122). PMID: [26101870](https://pubmed.ncbi.nlm.nih.gov/26101870/)
3. Diehl F, Schmidt K, Choti MA, Romans K, Goodman S, et al. (2007) Circulating mutant DNA to assess tumor dynamics. *Nat Med* 14: 985-990. doi: [10.1038/nm.1789](https://doi.org/10.1038/nm.1789). PMID: [18670422](https://pubmed.ncbi.nlm.nih.gov/18670422/)

4. Atkinson MA, Eisenbarth GS, Michels AW (2013) Type 1 diabetes. *Lancet* 383: 69-82. doi: [10.1016/S0140-6736\(13\)60591-7](https://doi.org/10.1016/S0140-6736(13)60591-7). PMID: [23890997](https://pubmed.ncbi.nlm.nih.gov/23890997/)
5. Herold KC, Usmani-Brown S, Ghazi T, Lebastchi J, Beam CA, et al. (2015)  $\beta$  cell death and dysfunction during type 1 diabetes development in at-risk individuals. *J Clin Invest* 125: 1163-1173. doi: [10.1172/JCI78142](https://doi.org/10.1172/JCI78142). PMID: [25642774](https://pubmed.ncbi.nlm.nih.gov/25642774/)
6. Husseiny MI, Kaye A, Zebadua E, Kandeel F, Ferreri K (2014) Tissue-specific methylation of human insulin gene and PCR assay for monitoring beta cell death. *PLoS One* 9: doi: [10.1371/journal.pone.0094591](https://doi.org/10.1371/journal.pone.0094591). PMID: [24722187](https://pubmed.ncbi.nlm.nih.gov/24722187/)
7. Fisher MM, Watkins RA, Blum J, Evans-Molina C, Chalasani N, et al. (2015) Elevations in Circulating Methylated and Unmethylated Preproinsulin DNA in New-Onset Type 1 Diabetes. *Diabetes* 64: 3867-3872. doi: [10.2337/db15-0430](https://doi.org/10.2337/db15-0430). PMID: [26216854](https://pubmed.ncbi.nlm.nih.gov/26216854/)
8. Akirav EM, Lebastchi J, Galvan EM, Henegariu O, Akirav M, et al. (2011) Detection of  $\beta$  cell death in diabetes using differentially methylated circulating DNA. *Proc Natl Acad Sci U S A* 108: 19018-19023. doi: [10.1073/pnas.1111008108](https://doi.org/10.1073/pnas.1111008108). PMID: [22074781](https://pubmed.ncbi.nlm.nih.gov/22074781/)
9. Lehmann-Werman R, Neiman D, Zemmour H, Moss J, Magenheimer J, et al. (2016) Identification of tissue-specific cell death using methylation patterns of circulating DNA. *Proc Natl Acad Sci U S A* 113: doi: [10.1073/pnas.1519286113](https://doi.org/10.1073/pnas.1519286113). PMID: [26976580](https://pubmed.ncbi.nlm.nih.gov/26976580/)
10. Fisher MM, Perez Chumbiauca CN, Mather KJ, Mirmira RG, Tersey SA (2013) Detection of islet  $\beta$ -cell death in vivo by multiplex PCR analysis of differentially methylated DNA. *Endocrinology* 154: 3476-3481. doi: [10.1210/en.2013-1223](https://doi.org/10.1210/en.2013-1223). PMID: [23825129](https://pubmed.ncbi.nlm.nih.gov/23825129/)
11. Pohl G, Shih I (2004) Principle and applications of digital PCR. *Expert Rev Mol Diagn* 4: 41-47. doi: [10.1586/14737159.4.1.41](https://doi.org/10.1586/14737159.4.1.41). PMID: [14711348](https://pubmed.ncbi.nlm.nih.gov/14711348/)
12. Sanders R, Huggett JF, Bushell CA, Cowen S, Scott DJ, et al. (2011) Evaluation of digital PCR for absolute DNA quantification. *Anal Chem* 83: 6474-6484. doi: [10.1021/ac103230c](https://doi.org/10.1021/ac103230c). PMID: [21446772](https://pubmed.ncbi.nlm.nih.gov/21446772/)
13. Vogelstein B, Kinzler KW (1999) Digital PCR. *Proc Natl Acad Sci U S A* 96: 9236-9241. PMID: [10430926](https://pubmed.ncbi.nlm.nih.gov/10430926/)
14. Gu J, Zang W, Liu B, Li L, Huang L, et al. (2017) Evaluation of digital PCR for detecting low-level EGFR mutations in advanced lung adenocarcinoma patients: a cross-platform comparison study. *Oncotarget* 8: 67810-67820. doi: [10.18632/oncotarget.18866](https://doi.org/10.18632/oncotarget.18866). PMID: [28978074](https://pubmed.ncbi.nlm.nih.gov/28978074/)
15. Allouchery V, Beaussire L, Perdrix A, Sefrioui D, Augusto L, et al. (2018) Circulating ESR1 mutations at the end of aromatase inhibitor adjuvant treatment and after relapse in breast cancer patients. *Breast Cancer Res* 20: 40. doi: [10.1186/s13058-018-0968-0](https://doi.org/10.1186/s13058-018-0968-0). PMID: [29769099](https://pubmed.ncbi.nlm.nih.gov/29769099/)
16. Selvaraj V, Maheshwari Y, Hajeri S, Chen J, McCollum TG, et al. (2018) Development of a duplex droplet digital PCR assay for absolute quantitative detection of "Candidatus Liberibacter asiaticus". *PLoS One* 13: doi: [10.1371/journal.pone.0197184](https://doi.org/10.1371/journal.pone.0197184). PMID: [29772016](https://pubmed.ncbi.nlm.nih.gov/29772016/)
17. Farr RJ, Januszewski AS, Joglekar MV, Liang H, McAulley AK, et al. (2015) A comparative analysis of high-throughput platforms for validation of a circulating microRNA signature in diabetic retinopathy. *Sci Rep* 5: 10375-1038. doi: [10.1038/srep10375](https://doi.org/10.1038/srep10375). PMID: [26035063](https://pubmed.ncbi.nlm.nih.gov/26035063/)
18. Dong L, Meng Y, Sui Z, Wang J, Wu L, et al. (2015) Comparison of four digital PCR platforms for accurate quantification of DNA copy number of a certified plasmid DNA reference material. *Sci Rep* 5: 13174. doi: [10.1038/srep13174](https://doi.org/10.1038/srep13174). PMID: [26302947](https://pubmed.ncbi.nlm.nih.gov/26302947/)
19. Alikian M, Whale AS, Akiki S, Piechocki K, Torrado C, et al. (2016) RT-qPCR and RT-Digital PCR: A Comparison of Different Platforms for the Evaluation of Residual Disease in Chronic Myeloid Leukemia. *Clin Chem* 63: 525-531. doi: [10.1373/clinchem.2016.262824](https://doi.org/10.1373/clinchem.2016.262824). PMID: [27979961](https://pubmed.ncbi.nlm.nih.gov/27979961/)
20. Bosman KJ, Nijhuis M, van Ham PM, Wensing AMJ, Vervisch K, et al. (2015) Comparison of digital PCR platforms and semi-nested qPCR as a tool to determine the size of the HIV reservoir. *Sci Rep* 5: 13811. doi: [10.1038/srep13811](https://doi.org/10.1038/srep13811). PMID: [26350506](https://pubmed.ncbi.nlm.nih.gov/26350506/)
21. Lee H, Park Y, We Y, Han DJ, Seo J, et al. (2017) Evaluation of Digital PCR as a Technique for Monitoring Acute Rejection in Kidney Transplantation. *Genomics Inform* 15: 2-10. doi: [10.5808/GI.2017.15.1.2](https://doi.org/10.5808/GI.2017.15.1.2). PMID: [28416944](https://pubmed.ncbi.nlm.nih.gov/28416944/)

## Supplementary information

**Figure S1.** Overview of two digital PCR platforms.

Supplementary information of this article can be found online at <http://www.jbmethods.org/jbm/rt/suppFiles/280>.